Electroencephalography and clinical Neurophysiology, 1990, 76: 540–556
Elsevier Scientific Publishers Ireland, Ltd.

EEG 89106

Representation of multi-channel evoked potential data using a dipole component model of intracranial generators: application to the auditory P300 [1]

Bruce Turetsky [a], Jonathan Raz [b] and George Fein [b]

[a] *Medical College of Pennsylvania and Eastern Pennsylvania Psychiatric Institute, Philadelphia, PA (U.S.A.), and* [b] *University of California and Veterans Administration Medical Center, San Francisco, CA (U.S.A.)*

(Accepted for publication: 23 January 1990)

Summary A number of procedures have been employed to decompose recorded scalp potential wave forms into their hypothesized constituent elements. The shortcomings of the various decomposition methods (principal components analysis, topographic components modeling, inverse dipole localization and spatio-temporal dipole modeling) are reviewed and a new dipole components model, which incorporates the strengths of the topographic components model and the spatio-temporal dipole model, is presented. This model decomposes ERPs into subcomponents reflecting the activity of dipole sources with location and orientation fixed across subjects and with the temporal activity of each dipole modeled as a decaying sinusoid. The requirement that the equivalent dipole generators be the same across subjects and experimental conditions permits analysis of inter-group differences and of the effects of experimental variables. An application of the model to data from a 3-tone auditory target detection task is presented, and equivalent dipole sources of the components of the auditory evoked potential are described. Assumptions inherent in the model, as well as practical obstacles to its widespread implementation, are discussed.

Key words: Dipole; Source localization; Auditory evoked potentials; Intracranial generators; P300; Components

Average event related potential (ERP) data from a typical experiment comprise a massive multi-dimensional array of electrical potential differences sampled from multiple scalp sites at many instants in time for each subject and experimental condition. Efforts to reduce this mass of data to a set of valid summary measures have been motivated by two complementary but distinct objectives: (1) to relate observed differences in ERPs to differences in clinical, demographic, or experimental task variables and (2) to relate scalp recordings to underlying neurophysiological activity. Different data reduction methods have tended to emphasize one or the other of these goals. Traditional peak-picking uses latencies and amplitudes of peaks and troughs at various individual electrode sites as summary measures for comparison across subgroups or tasks. Peak-picking rests on the tenuous assumption that the entire wave form can be adequately summarized by these point measures, with each deflection representing the latency and amplitude of peak activity of one subcomponent of the ERP. The latencies and amplitudes of comparable peaks and troughs, however, vary across recording channels and are dependent upon both the recording montage and the reference (Lehmann and Skrandies 1984). Further, there has been increasing recognition that the peaks and troughs seen in scalp recordings are composite representations of the temporally overlapping activity arising from multiple sources (e.g., Squires et al. 1975; Näätänen and Picton 1987). A number

[1] This work was supported by Veterans Administration General Medical Research Funds and a Veterans Administration Psychiatric Research Training Grant.

Correspondence to: George Fein, Ph.D., Veterans Administration Medical Center (116R), 4150 Clement Street, San Francisco, CA 94121 (U.S.A.).

of other procedures have been employed to extract neurophysiologically distinct subprocesses from scalp recordings, while also reducing the mass of data. However, none of these methods is entirely satisfactory. In this paper, we will briefly review some of the shortcomings of various techniques, and then present a dipole components model which, we believe, overcomes many of the limitations of previous decomposition strategies.

Principal components analysis (PCA) examines the variability of the recorded wave forms across subjects, conditions, and electrodes to decompose the scalp potentials into subunits called factors (Donchin and Heffley 1978). Each recorded time series is treated as a separate observation. The factors extracted by PCA are orthogonal time functions defined over the entire ERP epoch representing independent sources of variance in the data set; the number of factors reflects the dimensionality of this variance. Each ERP wave form is a weighted sum of the PCA factors, plus residual noise.

PCA has recently been used to decompose ERPs into orthogonal spatial factors (Skrandies and Lehmann 1982; Maier et al. 1987). In spatial PCA, each observation consists of the multichannel data recorded at a single instant in time; variation in scalp topography is used to identify factors which represent independent sources of variance in the topographic distribution of scalp potentials. Spatial PCA is based on a model wherein each underlying EP source produces a characteristic electrical field topography over the scalp.

However, PCA has limitations that apply equally to both the time series and spatial variants. First, variance is treated uniformly, regardless of its source. There is no difference in the treatment of (1) variance among the multiple electrodes (or time points in spatial PCA), (2) variance due to correlated residual noise, (3) between-subject variance, and (4) variance between experimental conditions. Second, PCA solutions are not unique, since equivalent solutions can be obtained by any rotation of the factors which maintains their dimensionality. Each rotation yields a different set of factors and a different allocation of variance amongst the new factors. The Varimax rotation, in which the factors must be orthogonal and the weightings for each factor across time points (or electrodes) are as close to 0 or 1 as possible, is used most commonly. When applied to simulated data sets with overlapping components, it produces factors that do not acurately reflect the true underlying components (Lutzenberger et al. 1981; Rösler and Manzey 1981; Wood and McCarthy 1984; Möcks and Verleger 1986). Third, the constraints of PCA and rotation algorithms are unrelated to neurophysiological and biophysical constraints that must exist in ERP data. This makes it unlikely that the partitions of variance which result from PCA reflect neurophysiologically meaningful entities. In an effort to overcome this limitation, Maier et al. (1987) used an oblique rotation to optimally fit a current dipole source to the spatial features of each principal component. However, in a simulated study of activity from overlapping dipole sources, this procedure severely mislocated source position and misallocated temporal variance among sources (Achim et al. 1988a).

An alternative decomposition strategy, the topographic components model (TCM), has recently been proposed by Möcks (1988a,b). Like time series PCA, TCM assumes that recorded scalp potentials are the weighted sums of overlapping time functions. However, TCM treats each source of variance separately in determining the components which account for non-random variance in the data set. Like PCA, TCM generates components that are time functions defined over the entire ERP epoch. Unlike PCA, TCM generates a separate set of weights for each source of variance (electrode location, experimental condition, and subject) for each component. Each time function is thus associated with its own unique set of electrode weights. Each TCM component thereby has both a characteristic course of activity over time and a set scalp topography. This is consistent with traditional notions of an ERP component arising from a generator in the brain. TCM assumes that the same component structure (i.e., time functions and associated electrode weights) exists across all subjects and also across all conditions. Subjects (or conditions) differ from one another in terms of the relative contribution of each component to their ERP wave forms. Differences in component *latencies* across subjects

or conditions are not included in the model, which is an important limitation of TCA. (Latency differences are also ignored in PCA; see Möcks 1986, concerning the effects of latency shifts on the PCA factor structure.) However, TCM avoids many of the other problems inherent in PCA. The model permits the data to be decomposed using many fewer parameters, such that the underlying component structure is uniquely determined. There is no requirement in TCM that subcomponents be mutually orthogonal, and the uniqueness of the solution eliminates the need to arbitrarily select a rotation algorithm. Moreover, by providing a set of subject and condition weights for each component, comparisons of component activity across subjects or conditions can be readily made using a small number of summary measures. However, there is nothing inherent in TCM that makes reference to the neurophysiologic and biophysical constraints on ERPs.

A different approach to wave form decomposition has been to explicitly link ERPs to the underlying neuroanatomic substrate. This approach begins with the idea that surface recordings are a composite representation of the electrical activity of multiple neural sources in the brain. At any instant, each source has a unique location, orientation, and magnitude of electrical activity, which produces a unique distribution of potentials on the scalp, consistent with the laws of electrostatic field theory and volume conduction (Nunez 1981). The surface electrical potentials arising from these individual sources sum together to yield recorded scalp potentials. In order to compute the scalp potentials associated with a given source, certain assumptions must be made concerning the geometry and electrical conductivity of the head, and the electrical charge configuration of the source itself. Usually, the head is modeled either as a sphere with uniform conductivity throughout, or as 3 spherical shells representing brain, skull, and scalp, each with its own conductivity, and the charge configuration of each source is represented by an equivalent dipole (Kavanagh et al. 1978; Darcey et al. 1980; Wood 1982; Fender 1987). Application of the method typically involves determining the particular configuration of equivalent dipoles that provides the least-squares best fit between the recorded scalp potentials and the scalp potentials predicted from the dipole model.

In the simplest version of the dipole model, a separate set of equivalent dipoles are fitted to the multi-channel scalp recordings for each time point in the ERP epoch (e.g., Kavanagh et al. 1978; Fender 1987). One problem with this procedure is that the number of sources that can be included in the model is severely limited. A complete description of the location, orientation, and magnitude of a single dipole in spherical space requires 6 *df* to specify 6 independent parameters: 3 for location, 2 for orientation, and 1 for magnitude. However, the total number of degrees of freedom in an instantaneous set of scalp potentials is no more than the number of recording electrodes. Therefore, typically, no more than 2–3 simultaneously active dipoles can be determined, and, with 6 independent parameters for each dipole at each time point, little if any data reduction is achieved. Also, since the optimum number of dipoles, their locations, and their orientations are derived separately for each time point, there are no constraints placed on the way these parameters might vary from moment to moment. This could result in a set of solutions (one for each time point) that strains physiologic credibility.

The spatio-temporal dipole model (STDM) (Scherg and Von Cramon 1985, 1986; Scherg 1989), attempts to overcome some of the difficulties of the instantaneous dipole method. STDM assumes that recorded scalp potentials represent the summed activity of a finite number of equivalent dipoles, *and* that each equivalent dipole has a fixed location and orientation that cannot vary over the course of the ERP epoch. Only the magnitude of the electrical activity of each dipole is allowed to vary over time. The contribution of a dipole to the time-dependent scalp potential at a given electrode site is computed by multiplying the dipole magnitude, which is a continuous time function, by an electrode-specific weight. Electrode weights are determined by the location of the electrode relative to the location and orientation of the dipole, and reflect the volume conduction of electrical potential from the dipole to the scalp. The working model of the generation of ERPs is that dipole sources remain anatomically

fixed from moment to moment. The location and orientation of the dipole reflects the spatial organization of the underlying neural structure, while the temporal course of the dipole magnitude reflects the structure's compound discharge processes (Scherg and Von Cramon 1985). Given fixed dipole position and orientation across the epoch, dipole activity for the entire ERP response can be characterized using far fewer variables than with instantaneous dipole methods. Thus, STDM can characterize many more overlapping generators; the only constraint is that the number of equivalent dipoles must be less than the number of recording electrodes (Scherg 1989).

There are a number of unresolved issues concerning the STDM. First, the dipole configuration that results from the STDM depends upon the constraints placed on the dipole magnitude time functions (Scherg and Von Cramon 1986). In Scherg and Von Cramon's early study (1985), the time functions were constrained to resemble the biphasic curves that were being fitted (i.e., the auditory ERP N100 trough and P200 peak). The parametric form of this time function provided measures of dipole latency and amplitude. However, since the peaks and troughs of the ERP are composite and relative phenomena (i.e., they reflect the activity of multiple sources and vary with the particular electrode montage and reference being used), the temporal activity of underlying sources need not be the same as that seen in scalp recordings. In subsequent work, Scherg and Von Cramon (1986) adopted a non-parametric model of dipole activity, avoiding arbitrary restrictions on the dipole magnitude function. The non-parametric time function, however, is more likely to be affected by noise in the data and also does not yield summary measures of dipole activity. Since there may be as many dipole wave forms as scalp electrode recordings, data reduction may be minimal. Further, there is no obvious way to analyze the STDM results.

Second, STDM examines the average evoked potentials (AEPs) of each subject separately; the resulting equivalent dipole sources are subject-specific. However, AEP wave forms contain, in addition to a composite signal, residual noise that may be highly correlated across both time and space. If the signal-to-noise ratio (SNR) is low, the noise may account for a substantial proportion of the overall variance. Unless additional constraints are imposed, such as assuming that the dipole structure is the same across subjects, the correlation structure of the noise in each subject's data can strongly affect the positions and orientations of the dipoles that are fitted (Darcey et al. 1980). Position and orientation parameters are also affected by the unique skull shape, skull thickness, and brain morphology of each subject (Ary et al. 1981), and dipole activity may not be well correlated with scalp amplitude across individuals. Consequently, STDM results may vary across subjects, and it is unclear how to compare results for different individuals. There is no objective procedure for deciding whether dipoles from 2 subjects represent the same or different underlying brain processes, when their defining parameters are not identical.

Finally, even if we assume that dipoles can be validly matched across subjects or conditions (i.e., that 2 dipoles reflect the same brain process), there is still the need for summary measures of dipole activity to use in examining experimental effects. The dipole components model, which we describe, is computationally very intensive but addresses many of the issues we have raised above. The model combines the strengths of TCM and STDM. It provides a basis for the partitioning of ERPs into neurophysiologic subunits, while also permitting unambiguous comparisons across subjects and conditions and effectively reducing the mass of data to a small number of parameters.

The essential features of the model are:

(1) Components are assumed to arise from equivalent dipole sources, with locations and orientations that remain fixed throughout the ERP epoch. Scalp potentials are determined by the biophysical constraints associated with volume conduction of dipole source activity in a homogeneous spherical medium.

(2) The time functions which describe dipole activity are given a parametric form. The entire time course of each dipole is thus represented by a few simple parameters, including both onset latency and magnitude of dipole activity.

(3) The underlying component structure is as-

sumed to be uniform across all data sets. In this sense, the model represents a particular application of the TCM framework. Subject and condition effects are included as modifying factors within this structure.

(4) Variations in component latency across subjects and conditions are explicitly incorporated as parameters in the model.

We will first describe the model in detail, and then present an application to data from a 3-tone auditory target detection task.

The dipole component model

Using the TCM framework of a uniform underlying component structure, we start with the assumption that the electrical potential at time t at electrode l, x(t, l), is equal to the weighted sum of K components. Each component, k, has a characteristic time function, $c_k(t)$, and a component-specific set of electrode weights, $b_k(l)$ (Scherg and Von Cramon 1986; Achim et al. 1988a; Möcks 1988a,b):

$$x(t, l) = \sum_{k=1}^{K} c_k(t) b_k(l) \quad (1)$$

Because each component is assumed to represent the activity of a single equivalent dipole source in a homogeneous spherical conducting medium, $b_k(l)$ is a non-linear function of electrode location and the position parameters (r, θ, ϕ in spherical coordinates) and orientation parameters (ψ_1, ψ_2) of each dipole (Brody et al. 1973).

The time functions, $c_k(t)$, which represent the electrical outputs of the neural networks that underlie each component, are modeled as decaying sinusoids of the following form:

$$c_k(t) = \alpha_k \sin\left[\frac{2\pi}{\lambda_k}(t - \tau_k)\right] e^{-\beta_k(t-\tau_k)}, \; t \geq \tau_k \quad (2)$$

This function has 4 parameters: (1) τ_k is the onset latency; output is assumed to be 0 for $t < \tau_k$; (2) α_k is a measure of the output amplitude; (3) λ_k is the output oscillation wavelength ($2\pi/\lambda_k$ is the oscillation frequency); (4) β_k is the oscillation decay rate. Using this parametric model, the entire output function of each equivalent dipole is represented by 4 numbers, with unambiguous measures of the latency and amplitude of the equivalent dipole's output.

Inter-subject differences in dipole output amplitude and latency are incorporated into the model. Amplitude differences among subjects (i) for each component are specified via subject-specific weights, $a_k(i)$ (Möcks 1988a,b), with:

$$x(t, l, i) = \sum_{k=1}^{K} c_k(t) b_k(l) a_k(i) \quad (3)$$

Latency differences among subjects are incorporated using subject-specific latency shifts, τ_{ki}, which modify $c_k(t)$, resulting in:

$$c_k(t, i) = \alpha_k \sin\left[\frac{2\pi}{\lambda_k}(t - \tau_k - \tau_{ki})\right] e^{-\beta_k(t-\tau_k-\tau_{ki})} \quad (4)$$

To ensure uniqueness, the subject weights, $\alpha_k(i)$, are scaled to have a product of 1, and the latency shifts, τ_{ki}, are adjusted to have a mean of 0 for each equivalent dipole.

Differences across experimental conditions are treated in an analogous fashion: (1) the underlying component structure is modified by a set of condition-specific weights, $e_k(m)$, and (2) the latency of each component is adjusted by a condition-specific latency shift, τ_{km}, with the same uniqueness constraints on $e_k(m)$ and τ_{km} as for the subject parameters. The final dipole component model takes the following form:

$$x(t, l, i, m) = \sum_{k=1}^{K} \alpha_k \sin\left[\frac{2\pi}{\lambda_k}(t - \tau_k - \tau_{ki} - \tau_{km})\right] \times e^{-\beta_k(t-\tau_k-\tau_{ki}-\tau_{km})} b_k(l) a_k(i) e_k(m), \quad (5)$$

where x(t, l, i, m) represents the average evoked potential at time t from electrode l, for the i-th subject during the m-th experimental condition, and the topographic weights, $b_k(l)$, are determined by the positions and orientations of the underlying sources.

To compute the values of these parameters for a real data set, we model the head as a homogeneous sphere and employ an iterative simplex

convergence procedure in which all of the parameters for each dipole are adjusted simultaneously, in order to minimize the difference between the predicted and recorded potentials (O'Neill 1971). The predicted scalp potentials associated with each dipole source are *reference-free* measures. To compare the model wave forms with actual scalp recordings, each is converted to an average reference format (Scherg and Von Cramon 1985). The fit of the model to the data is then measured by the sum of squared differences between the estimated and real potentials, across all subjects, conditions, and electrodes. The fitting procedure can be computationally very intensive, depending on the total number of parameters in the model (which is a function of the number of different dipoles, conditions, and subjects in the data set), the number of electrodes and time points being fitted, and the hardware being used for implementation.

Dipole component representation of auditory evoked potential data

To demonstrate the use of the dipole component model, we apply it to a set of ERP data collected from a group of normal subjects, during a moderately difficult auditory target detection experiment.

Methods

Subjects

Healthy individuals between the ages of 21 and 38 years were recruited from the community. Subjects were excluded if there was a history of previous medical or neuropsychiatric illness, substance abuse, head injury, or hearing difficulties. Twenty-one subjects were studied, but the ERP data from 3 individuals were contaminated by electrical artifacts and could not be used. The final sample of 18 consisted of 12 males and 6 females, aged 22–38 years.

Experimental procedure

In order to standardize target detection task difficulty, we first determined each subject's threshold for discriminating between a 1000 Hz tone and a second tone of higher frequency. An alternating ascending and descending 'method of limits' procedure was used with a forced-choice 'same' or 'different' response required. Throughout all procedures, tones were presented binaurally through headphones at 50 dB. The mean threshold frequency for 50% correct discrimination was 1017.5 Hz (S.D. = 18.5 Hz).

Subjects were then presented with a random series of tones of varying frequency, with a constant stimulus duration of 40 msec. The interstimulus interval varied randomly between 1.5 and 1.6 sec. Seventy percent of the tones were 1000 Hz 'standard' tones; 15% were 950 Hz, designated as a rare 'non-target'; the remaining 15% were higher frequency 'target' tones, to which subjects responded by lifting the right index finger. The actual target frequency was independently set for each subject, based on the threshold discrimination frequency. The difference between the target and the 1000 Hz standard was 4 times that of the threshold frequency (e.g., if the threshold frequency were 1015 Hz, then the target frequency was 1060 Hz).

ERP recordings

Electrodes were applied at Fpz, Fz, Cz, Pz, and Oz. Four additional electrodes were placed along the midline, midway between the following pairs: Fpz and Fz, Fz and Cz, Cz and Pz, Pz and Oz. This montage provided a chain of 9 equidistant electrodes overlying the mid-sagittal plane. All scalp electrodes were referenced to the left ear, A1. The electro-oculogram (EOG) was recorded between 2 electrodes placed above the left outer canthus and below the right outer canthus. EEG and EOG were amplified with a Grass Model 7B polygraph (60 Hz filter, band pass = 0.1–35 c/sec). Each channel of EEG was sampled every 4 msec, from 40 msec pre-stimulus to 760 msec post-stimulus. The data for any single trial was rejected if the EOG was greater than 35 μV baseline-to-peak or if there was A/D converter saturation (+/− 125 μV).

Stimuli were presented until 32 correctly classified trials without EOG artifact or A/D saturation were recorded for both the rare non-target and target conditions. Average wave forms were

computed from the single trials for each subject and condition, and smoothed using a kernel smoother with an order 4 kernel (Gasser and Müller 1979). For each wave form, the smoothing parameter was selected to minimize the estimated mean average square error (Hart and Wehrly 1986; Raz et al. 1989).

Implementation of the dipole model in two dimensions

The head was assumed to be a homogeneous sphere with unit radius and uniform electrical conductivity. A mid-line sagittal cross-section through the chain of recording electrodes thus defined a unit circle within an anterior-posterior plane. Since we had no information concerning the lateral distribution of scalp potentials, we restricted the analysis to this two-dimensional model projection of the head. Within this plane of analysis, the location of each electrode was specified by a pair of polar coordinates (r, θ), where r represented the distance from the center of the unit circle (in this case, 1.0 at the circumference) and θ represented the angle of displacement from the horizontal axis (defined as 0° at Fpz and 180° at Oz). The projection, in the mid-sagittal plane, of the location of each equivalent dipole source could be similarly specified by the two parameters r and θ, with $0 \leqslant r < 1$ and $-180° \leqslant \theta \leqslant +180°$. The orientation of each dipole required a third parameter, ψ, the angle of orientation, defined according to the same coordinate axes as the angle of displacement (Fig. 1). Dipole components were determined for the time epoch from stimulus onset to 400 msec post-stimulus presentation.

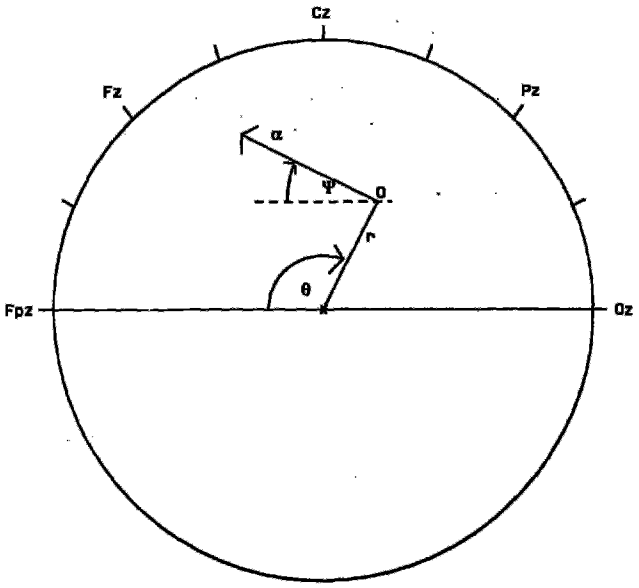

Fig. 1. Spherical coordinate system used to represent dipoles in the mid-sagittal plane. The location of the dipole at point O is expressed by 2 parameters: the angle θ and the distance from the center, r. Dipole orientation is given by the angle ψ. The magnitude of dipole activity, α, is represented by the length of the dipole.

Results

The grand average ERPs, for each of the 3 conditions, are presented in Fig. 2 as average-referenced spatio-temporal contour plots (Rémond 1968). These plots illustrate the typical morphology of the auditory evoked potentials obtained in a rare target detection task: an N100-P200 complex is followed by a P300 positive peak, which is greatest over the central and parietal electrodes for the target condition, but smaller and more frontal in the standard and non-target wave forms. Fig. 3 presents a random selection of 4 target AEPs from individual subjects. It illustrates the tremendous differences in wave form morphology that exist between subjects. It is important to recognize the extent of this inter-subject variability in the data, since the dipole component model extracts a set of common underlying components. Variations that cannot be incorporated into this uniform component structure, (e.g., single-electrode artifacts or differences arising from inter-subject variation in the location of equivalent dipole sources or in brain and head morphology) contribute to the unexplained residual variance.

To determine an appropriate number of components to include in the model, damped sinusoidal dipoles were initially fitted to the grand average data. Table I lists the proportion of total variance of the grand averages explained by the dipole model, assuming different numbers of underlying components (Scherg and Von Cramon 1985). The amount of explained variance is listed separately for each condition, as well as for the

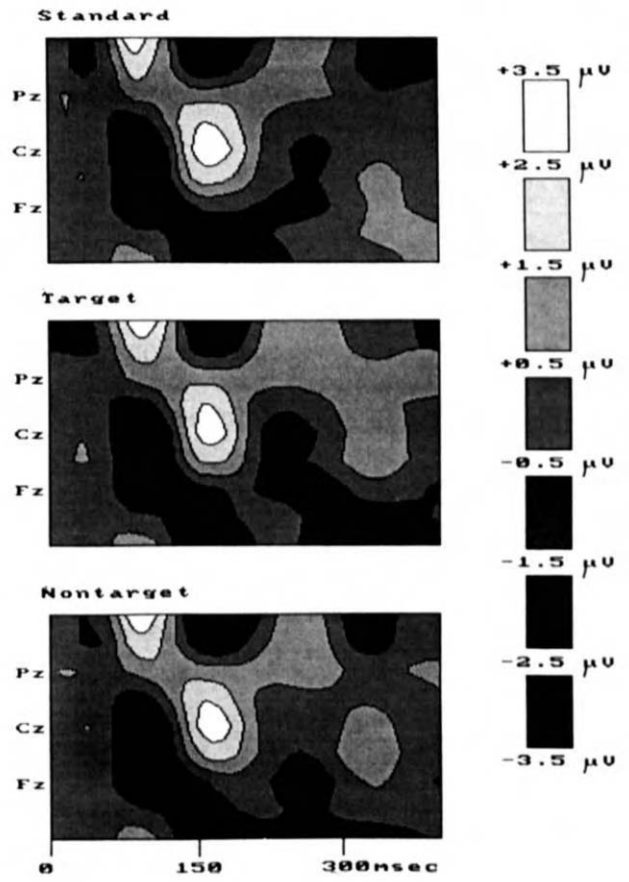

Fig. 2. Grand average ERP data from 18 subjects, presented separately for the standard, target and rare non-target conditions. Individual subject data were smoothed prior to averaging, using an order 4 kernel smoother that minimized the estimated mean average square error. Each plot presents the average-referenced electrical potentials at 9 midline electrode sites, from stimulus onset to 400 msec post stimulus. The x-axis represents time from stimulus onset; the y-axis represents the anterior-posterior scalp location. The different shaded contour regions correspond to different electrical potentials, according to the grey scale on the right.

total data set. A 3-dipole model was able to account for more than 91% of the variance across all 3 conditions and all 9 electrodes. A 4-dipole model explained only 1% more of the total variance, and the injection of a fifth dipole into the model also failed to add appreciably to the amount of variance explained for any condition. However, examination of the residual wave forms from the 3-dipole model revealed a series of small peaks and troughs that were localized both temporally and spatially, yet were not being accounted for by the model. The fourth dipole fitted these peaks and troughs. The residual wave forms from the 4-dipole model, in contrast, contained only random fluctuations, and the fifth dipole in the 5-dipole model, appeared to be fitting only low-amplitude residual noise. We therefore chose to apply a 4-component model to the entire set of AEPs from 18 subjects. The 4 decaying sinusoidal functions in this model accounted for 64% of the total variance across all subjects, electrodes, and conditions.

Description of the 4-dipole model

Positions and orientations of dipoles. Table II presents the 7 parameters that define each of the 4 equivalent dipoles (designated A–D). r and θ specify dipole positions in the mid-sagittal plane, while ψ specifies the initial *positive* direction of the dipole magnitude function. The position and orientation of each dipole, within the mid-sagittal unit circle, is depicted in Fig. 4. It is important to remember that (1) these position parameters are based on the assumptions of a spherical homogeneous conducting medium that is the same across subjects, and (2) since we do not have recordings from lateral electrode sites, it is impossible to differentiate between deep midline and lateralized peripheral locations.

Temporal and topographic characteristics of dipole source activity. With regard to the parameters (in Table II) specifying the damped sinusoidal output function of each equivalent dipole, τ_k is the onset latency (msec post-stimulus presentation); α_k is the amplitude; λ_k is the wavelength (msec); and β_k is the rate of decay. The τ_k

TABLE I

Percent of grand average variance explained by different numbers of dipoles.

No. of dipoles	Condition			
	Standard	Target	Rare non-target	Total
1	58.6	51.1	62.5	56.1
2	81.1	76.9	89.9	82.3
3	90.6	91.7	91.9	91.4
4	91.0	93.1	93.0	92.4
5	91.9	94.1	93.4	93.2

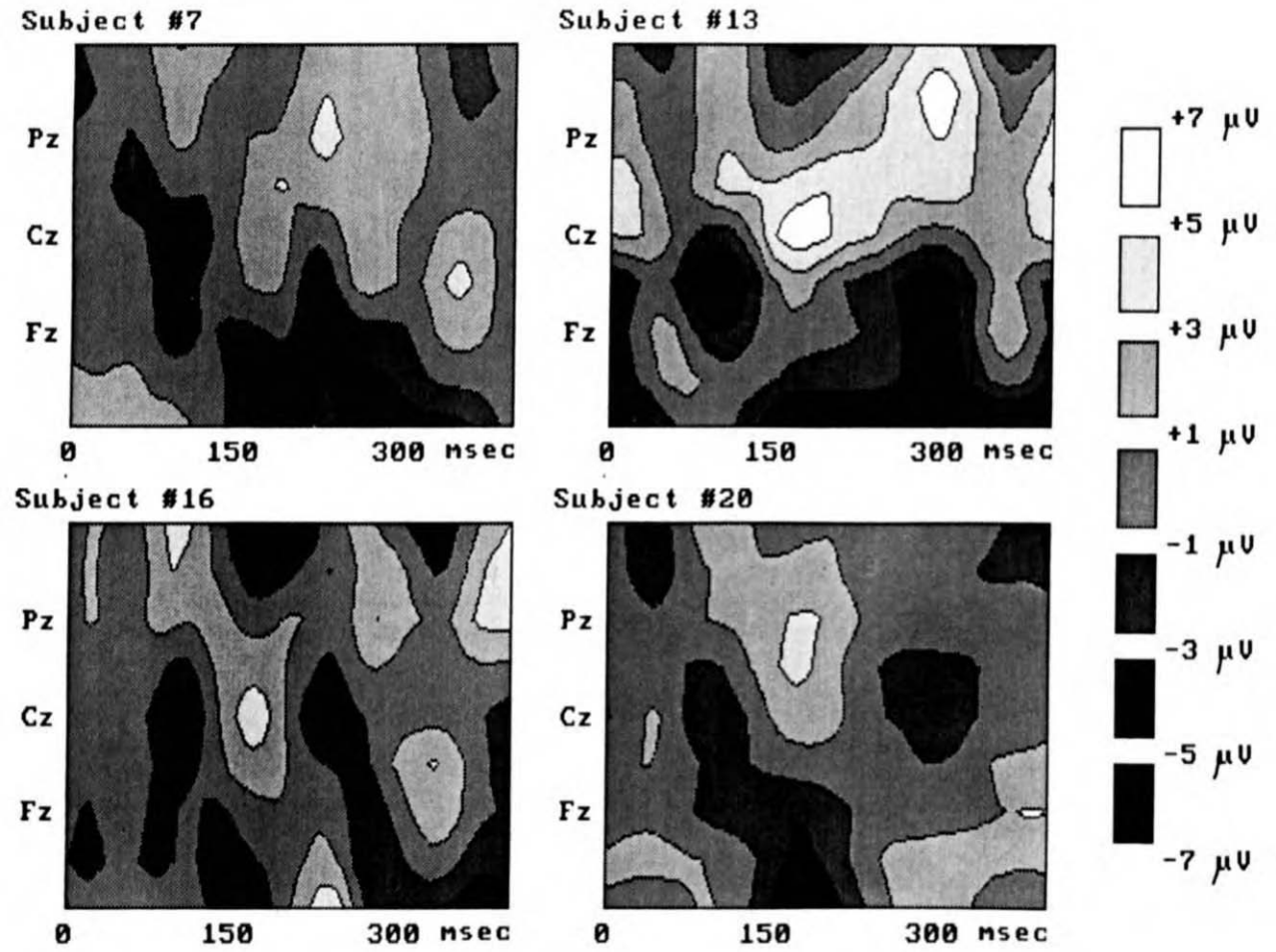

Fig. 3. Average-referenced spatio-temporal contour plots of the target response from 4 randomly selected subjects. Although the plots generally resemble the target grand average (Fig. 2), they illustrate the substantial inter-subject variability that exists in ERP morphology.

parameter reveals a clear sequencing of the activity of the 4 dipoles. The initial response is produced by dipole A, which becomes active at 63 msec post stimulus. This is followed by activation of dipole D at 95 msec, dipole B at 126 msec, and finally dipole C at 230 msec. Hypotheses regarding the neuroanatomic substrates and information processing functions of equivalent dipoles must be consistent with both their anatomic locations and timing.

The oscillating output of each dipole produces, through volume conduction, a similarly oscillating

TABLE II

Parameters of 4-dipole model.

Dipole	r	$\theta°$	$\psi°$	τ_k	α_k	λ_k	β_k
A	0.195	93.29	−105.90	63.26	15.04	159.72	0.0182
B	0.215	107.19	90.78	125.56	21.70	435.92	0.0699
C	0.088	176.90	171.17	229.76	22.79	1017.72	0.0529
D	0.290	93.50	123.49	95.48	6.39	176.16	0.0202

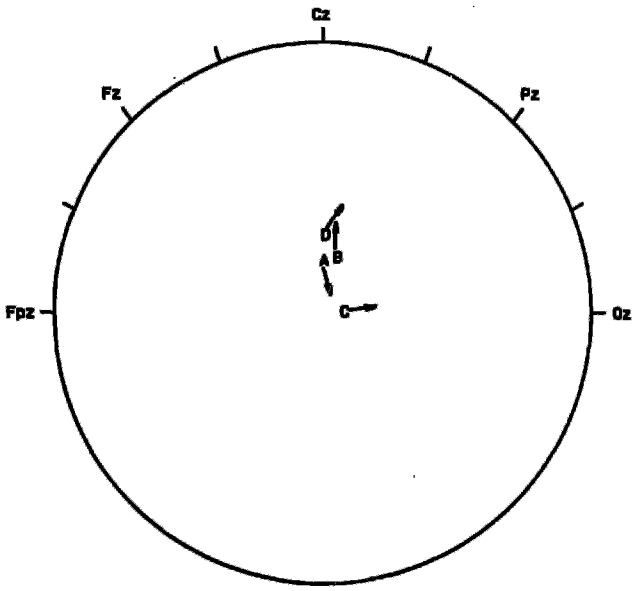

Fig. 4. Positions and orientations of 4 equivalent dipole sources of the auditory evoked potential, as defined by parameters in Table II. Each letter represents the location of 1 dipole. The adjacent arrow gives the orientation of initial positive activity. For each source, dipole position reflects the projection into the mid-sagittal plane. The midline electrode configuration does not permit a distinction between lateral and midline source locations.

electric field on the scalp surface. The electrical potential associated with this field has a characteristic topography, reflecting the position and orientation of the dipole, and a temporal pattern mirroring the activity of the dipole. Fig. 5 depicts the reference-free electrical potentials, along the midline chain of electrodes, produced by the activity of each of the 4 equivalent dipoles. This illustrates how the spatial and temporal parameters of each dipole translate into a distinctive set of scalp potentials, which represent the contribution of one source component to the total scalp ERP. It can be seen from the figure that dipole A, whose field strength is greatest near the Cz electrode, makes a substantial contribution to the vertex negative ERP around 100 msec, as well as to the positive peak around 200 msec. In addition, since the decay rate is relatively slow, this dipole also contributes to the later trough-peak configuration between 200 and 400 msec. Dipole B, in contrast, produces only a single centro-parietal peak of scalp activity, broadly spanning the neighborhood of 200 msec. Dipole C, with its later onset and orientation parallel to the Fpz-Oz axis, produces a low-frequency peak between 300 and 400 msec, that is positive posteriorly between Pz and Oz, but negative frontally. Dipole D also affects the anterior and posterior scalp areas differently. Its main contribution is a centro-parietal peak between 100 and 200 msec, with a smaller associated anterior trough. The composite ERP at each electrode site is simply the sum of the overlapping activities of these individual components. This composite model ERP is depicted in Fig. 6, as an average-referenced contour plot for each of the 3 conditions. The 4 dipole components combine to produce a scalp ERP that includes all of the characteristic peaks and troughs that one sees in an auditory target-detection experiment (as in Fig. 2).

Experimental condition effects

Table III presents the set of condition weights, $e_k(m)$, and the condition-specific latency shifts, τ_{km}, that were used to modify the underlying component structure for each of the 3 experimental conditions. The latency parameter, $\tau_{k,m}$, is measured in msec and represents the shift in the onset latency of each dipole; a positive value represents a slowing, while a negative value indicates a speeding of the onset of dipole activity. To assess whether the variation in each of these parameters was merely random, or whether it represented a real difference in dipole activity across conditions, we performed a randomization test on the data. For each subject, the 3 sets of average evoked potentials (1 for each of the 3 experimental conditions) were randomly assigned to the 3 different condition categories. The 2 condition parameters for each dipole, $e_k(m)$ and τ_{km}, were then recomputed from the complete data set with the randomly assigned conditions. We repeated this randomization and recomputation procedure 135 times, obtaining a distribution of condition parameters under the null hypothesis that differences between conditions are random with mean zero in the population. We were then able to compare the actual parameters we obtained with the null hypothesis distribution. As test statistics, we computed the variance of the latency and the variance of the log of the amplitude across conditions, and

TABLE III

Condition-specific amplitude and latency parameters.

Condition	Dipole							
	A		B		C		D	
	e_k(m)	τ_{km}	e_k(m)	τ_{km}	e_k(m)	τ_{km}	e_k(m)	τ_{km}
Standard	0.96	+1.17	1.05	−7.12	0.68	−7.36	0.79	+0.15
Target	1.03	−1.12	0.89	+7.01	1.47	+15.73	1.26	+2.25
Rare non-target	1.02	−0.06	1.08	+0.11	1.00	−8.37	1.01	−2.40

estimated the probability of obtaining, by chance alone, values equal to or higher than those from our model when the true experimental conditions were assigned to the data. When the condition effect for a given parameter was significant ($P < 0.05$), we examined the paired contrasts between conditions to identify the source of the between-conditions variance.

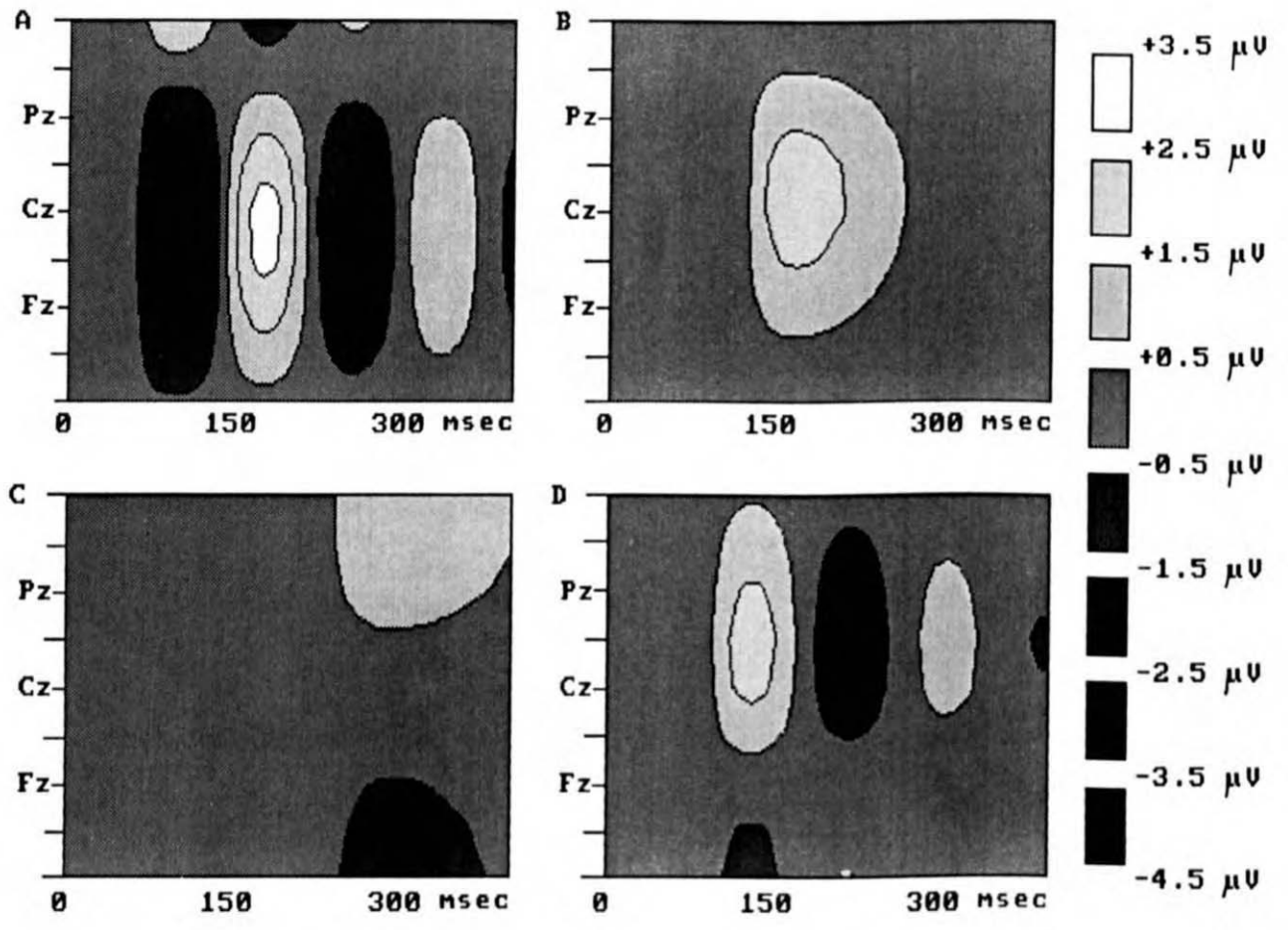

Fig. 5. Spatio-temporal contour plots of the midline scalp activity arising from each of 4 equivalent dipole sources. Each plot presents the reference-free electrical potential at 9 midline electrode sites, from stimulus onset to 400 msec post stimulus, prior to the inclusion of condition-specific or subject-specific latency and amplitude parameters.

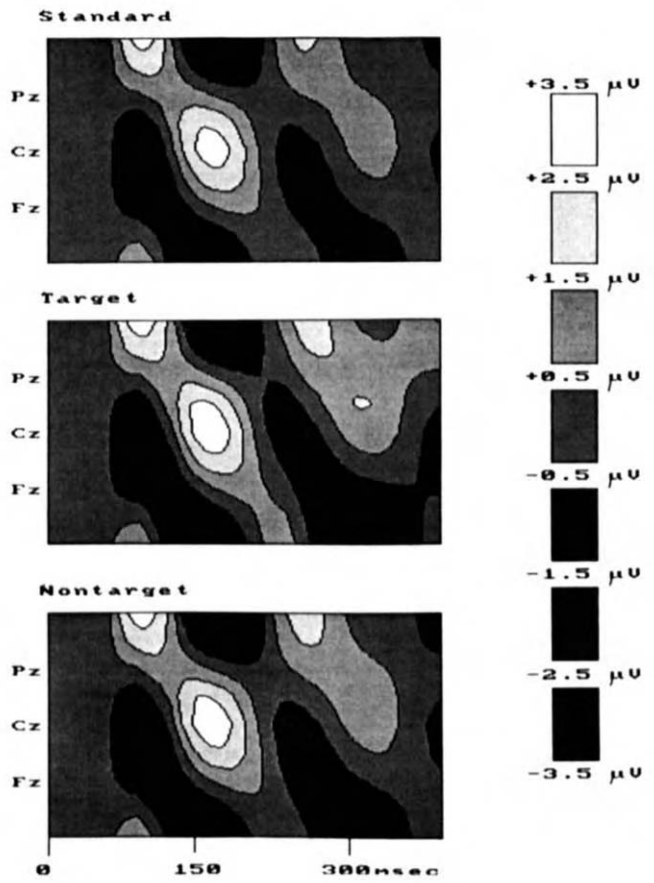

Fig. 6. Spatio-temporal contour plots depicting the composite average-referenced scalp activity from 4 equivalent dipole sources. The composite electrical potential is the sum of the potentials arising from each of the 4 dipoles displayed in Fig. 5, after modification of each dipole by its condition-specific latency and amplitude parameters and transformation to the average reference. Comparison between these plots and the grand averages presented in Fig. 2 illustrates the goodness of fit of the dipole component model.

There were significant differences across the 3 conditions for 3 of the 4 dipole amplitude parameters and for one of the latency parameters. Table IV summarizes these results, presenting the estimated probability for each of the 4 dipole amplitude and latency parameters, along with the paired contrasts of significant condition effects. It can be seen that dipole A did not differ in either amplitude or latency across the 3 conditions. There were significant amplitude differences for dipoles B, C, and D, and a significant latency shift for dipole C. Examination of the paired contrasts shows that,

TABLE IV

Tests of significance of condition-specific amplitude and latency parameters.

Parameter	Estimated P values			
	Dipole			
	A	B	C	D
$\ln e_k(m)$	0.215	0.022	0.007	0.007
Paired contrasts				
Standard vs. target		0.030	0.007	0.007
Standard vs. non-target		0.785	0.111	0.044
Target vs. non-target		0.007	0.111	0.044
τ_{km}	0.467	0.089	0.037	0.259
Paired contrasts				
Standard vs. target			0.052	
Standard vs. non-target			0.882	
Target vs. non-target			0.022	

for dipole B, the target was smaller than both the standard and the rare non-target, while these 2 conditions did not differ from each other. For dipole D, the target amplitude was greater than that of the non-target, the non-target amplitude was, in turn, greater than that of the standard. The amplitude pattern for dipole C was similar to that of D, however only the paired contrast between the target and standard tones had an estimated significance probability less than 0.05. The latency of dipole C was also significantly longer for the target tone than for the other 2 conditions.

Inter-subject variability

To examine the extent of the inter-subject variability that was present for each of the 4 dipoles, we computed the standard deviation, across subjects, of the subject-specific latency shift, τ_{ki}, and of the log of the subject amplitude parameter, $a_k(i)$. These are presented in Table V. The inter-subject variability in dipole parameters correlates

TABLE V

Standard deviation of subject-specific amplitude and latency parameters.

Parameter	Dipole			
	A	B	C	D
$\ln a_k(i)$	0.37	0.81	1.12	0.58
τ_{km}	10.84	49.93	75.81	32.67

directly with the temporal sequence of the 4 dipoles. The earliest dipole, A, exhibits the least variability, while the dipole with the latest onset, C, varies the most across subjects. This is consistent with the notion that the earliest ERP components reflect primary sensory processing of the physical features of stimuli, while later components reflect secondary cognitive processes which are likely to be much more variable from subject to subject. None of the subject parameters were related to subject age in this relatively homogeneous sample. There were, however, significant relationships between sex and the onset latencies of dipoles A and C, with earlier activity for females compared to males. For dipole A, the mean difference in latency shift between the sexes was 9.58 msec (3.20 + /− 11.76 S.D. for males versus −6.38 + /− 4.61 S.D. for females); t (16) = 2.47, P = 0.0256. The mean difference for dipole C was 95.84 msec (31.95 + /− 64.03 S.D. and −63.89 + /− 56.31 S.D. for males and females, respectively); t (16) = 3.11, P = 0.0068.

Dipole fitting of individual subject data

The dipole component model imposes a uniform component structure across all data sets. We examined the variability of the 4-dipole solution from subject to subject when this constraint was not imposed. For each subject, the same starting parameters for the 4 dipoles were used (Table II). This biased the iterative simplex procedure towards obtaining similar results across subjects. Fig. 7 illustrates the resulting dipoles and their between-subject variability in location and orientation. For the purpose of comparison, we equated dipoles from different subjects based on their starting parameters (A, B, C, or D). Despite the conservative approach of using identical starting parameters for each subject, only the earliest dipole, A, showed a tight clustering across subjects for both position and orientation. The other dipoles, especially dipole C with its late onset, showed marked between-subject variability in position and orientation.

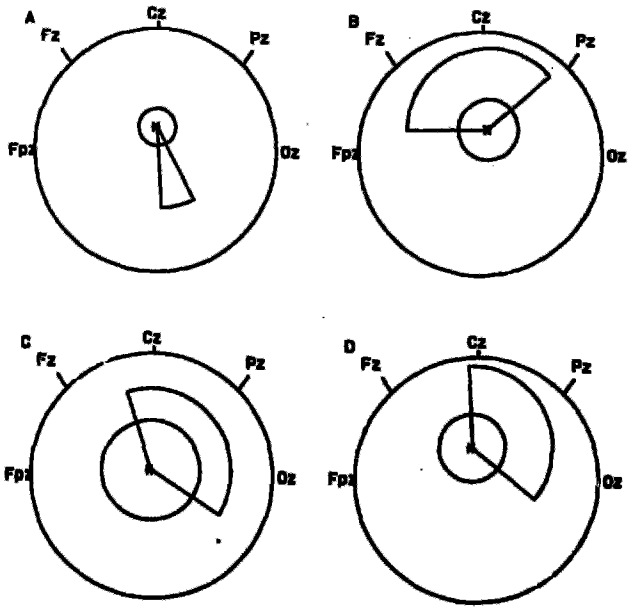

Fig. 7. Pictorial representation of the between-subject variability of position and orientation of the 4 dipoles, when the constraint of a uniform component structure is not imposed. For each dipole, * represents the mean location across 18 subjects. The radius of the surrounding circle denotes 1 S.D. of the Euclidean distance of individual subject dipole locations from this mean location. The pie-shaped sector represents +/−1 S.D. of the dipole orientations.

Table VI presents the means and standard deviations, across subjects, of the parameters of the decaying sinusoids. Dipoles B and D overlapped considerably on all 4 parameters. Since they also overlapped in position and orientation (Fig. 7), the result was an ambiguous situation in which

TABLE VI

Individual subject decaying sinusoid parameters. Values are means ± S.D.

Dipole	τ_k	α_k	λ_k	β_k
A	60.81 (7.44)	16.04 (5.23)	161.33 (18.18)	0.019 (0.017)
B	128.08 (56.60)	23.30 (20.34)	478.68 (295.24)	0.050 (0.035)
C	214.42 (97.00)	37.06 (46.79)	803.95 (341.30)	0.060 (0.032)
D	95.29 (48.28)	8.14 (6.15)	294.60 (413.79)	0.020 (0.017)

these 2 dipoles could not be uniquely matched across subjects. This difficulty is avoided by the constraints on both position and wave shape imposed by the dipole component model.

Discussion

The dipole component model is a general approach to the decomposition of scalp-recorded ERPs. The model accounts for data from multiple electrodes over an entire recording interval using a small number of parameters, while incorporating the laws of electrostatic field propagation that underlie ERP recordings. It holds the promise of decomposing observed scalp potentials into the contributions from multiple overlapping neural generators and providing clues to the locations of those generators. The requirement that component sources be the same across subjects and experimental conditions facilitates analysis of between-subject and within-subject experimental effects, and reduces the likelihood that the solution will be affected by residual noise.

The model, as we have presented it, assumes that the time functions of the underlying components are decaying sinusoids. This parametric representation yields unambiguous summary measures of large data sets, but it tightly constrains the temporal morphology of source activity. There is some physiological evidence to support the use of a decaying sinusoid to represent the output of an anatomically restricted neural aggregate, at least in the case of the rabbit bulbar cortex (Freeman 1975, 1980, 1985). However, the model is not dependent on a specific parametric representation of source activity; the particular form of the time function can be revised in response to accumulating data regarding underlying neurophysiology. What is important is the general approach of using such a parametric model.

When applied to data from an auditory target detection experiment, the model revealed that differences across experimental conditions resulted from differences in the activity of specific underlying dipole components. In this example, the model accounted for nearly two-thirds of the total variance across subjects, conditions, and electrodes. While this proportion of explained variance is low compared to the proportion of variance typically explained by PCA, our model is more parsimonious than PCA, it imposes reasonable physiological constraints as it reduces the data to an underlying component structure, and it extracts summary measures for statistical analyses. Given the tremendous variation across subjects of both physical features (e.g., head size, shape and skull thickness) and the morphology of scalp recordings, this proportion of explained variance, plus the significant experimental effects observed both within and across subjects, supports the strategy of assuming that a uniform component structure underlies the ERP wave forms.

However, the goodness-of-fit of the model could probably be improved by modifying its implementation in certain ways. Our experience fitting dipoles to single-subject data, as well as the experience of others (Scherg personal communication), suggests that intersubject variation in dipole orientation can be pronounced even when location is comparable. This, of course, simply reflects differences in the in-folding of cortical sulci. An additional parameter, reflecting differences in dipole orientation across subjects, could be readily incorporated into the model to account for such differences. The uniformity of the component structure across data sets would still remain with respect to anatomic location and the morphology of temporal activity. A second modification involves consideration of differences in noise power across subjects and electrodes. The least-squares minimization procedure gives equal weight to the recording at each electrode for each subject. Alternatively, one could compute a weighted least-squares fit, in which each average ERP recording is weighted by the reciprocal of its estimated residual noise power (Turetsky et al. 1988). 'Noisy' subjects and 'noisy' electrodes would then be given less consideration.

In our implementation of the dipole component method, we modeled the head as a homogeneous spherical conductor. This is, of course, imprecise. Because the skull has much lower conductivity than either brain matter or scalp (Nunez 1981), some investigators have instead used a 3-shelled spherical model of the head (Kavanagh et al.

1978; Scherg and Von Cramon 1985; Fender 1987). In practice, this has meant computing equivalent dipoles based on a homogeneous model, as we have done, and then estimating a correction factor to account for the decrease in skull conductivity. Interpolation tables are available (Ary et al. 1981) that match dipole locations from the homogeneous model with locations from the 3-shelled model, assuming 'standard' skull and scalp measurements. The main difference between the 3-shelled and homogeneous sphere models is that superficial dipoles appear to be situated further away from the scalp surface in the homogeneous conducting medium than in the 3-shelled inhomogeneous medium. Dipoles located closer to the center of the sphere are only minimally affected by differences in the two models (Ary et al. 1981; Nunez 1981). However, in simulation studies in which predicted dipole locations computed from the homogeneous model were compared to the actual locations of dipoles placed inside both a saline-filled sphere and a skull filled with saline and covered with a saline-soaked wool cloth, electrical inhomogeneities of the skull and scalp attenuated dipole magnitudes but did not increase the magnitude of error in the localization of dipole sources (Henderson et al. 1975).

It may be, therefore, that errors associated with other biases in the models outweigh the difference between the homogeneous and 3-shelled spherical models. Both of these models, for example, ignore deviations of head shape from true sphericity. An alternative approach has been to forsake the analytic expression of dipole potential afforded by a spherical model, in favor of a boundary element computation that incorporates the true shape of the head (He et al. 1987; Homma et al. 1987). Initial results with this method suggest that an accurate representation of head shape facilitates accurate dipole localization, even while assuming homogeneity of the conducting medium.

Another important issue for the application of the model is choosing the appropriate number of dipoles. If we use a very large number of dipoles, we will be able to fit the observed data very precisely. However, this is neither physiologically plausible nor practical. It also ignores the fact that the data contain residual noise, which we do *not* want to fit. In this paper, we chose the number of dipoles empirically by examining the residuals of the grand average wave forms (Scherg and Von Cramon 1985). Maier et al. (1987) employed a singular value decomposition method to address this question. Achim and associates have developed, for average ERP data from a single subject, a statistical test based on examination of the residual noise in single trials (Achim et al. 1988b). It is possible that an analogous test criterion could be developed for a multi-subject dipole component model. Another statistical approach to the problem could be derived by expressing the dipole model as a statistical model, defining a likelihood function, computing maximum likelihood estimators, and using a method such as the Akaike Information Criterion (AIC) to specify the model (Priestley 1981). This statistical approach probably would be easiest to implement in the frequency domain (Brillinger 1981; Möcks et al. 1988), in which maximum likelihood estimators could be constructed by weighted least squares, with the weights being inversely proportional to the noise power at a given frequency. One major advantage of a maximum likelihood model of dipole components, if it can be developed, would be estimation of variances and confidence intervals for the model parameters. This would eliminate the need for randomization tests.

We have limited ourselves to an application of the method to average evoked potential data from a homogeneous group of subjects. However, the model can be extended to both the study of group differences and to an analysis of single-trial data. When studying different subject groups, group or group-by-condition amplitude and latency shift parameters can be added to the model, analogous to our inclusion of subject-specific and condition-specific parameters. Single-trial components also might be modeled in the same way, with the addition of trial-specific amplitude and latency shift parameters. While the signal-to-noise ratio of single-trial data is an obvious problem, decomposition of the ERP wave form into equivalent dipole components provides additional information concerning the spatial distribution of each component of the signal embedded in the raw ERP recordings. This extra information regarding

the spatial dimension of the signal could increase the effective signal-to-noise ratio of the data, and facilitate the task of signal identification in the single-trial wave forms. Such an approach, if effective, would facilitate direct assessment of trial-to-trial variation in the latency and amplitude of individual subcomponents of the ERP.

A major impediment to the further development of these methods is their computational requirements. The convergence algorithms demand a great deal of processing time. Increasing the number of parameters in the model, by increasing the total number of dipoles, by fitting these dipoles in 3-dimensional space instead of two dimensions, by permitting dipole orientation to vary across subjects, or by adding single-trial parameters, would increase the length of time needed to converge to a solution. Similarly, enlarging the data set, either by increasing the number of subjects or conditions, by adding more electrodes, or by using single trials instead of averages, would also increase the computational demands on the convergence algorithm.

We have no doubt that the computational requirements will be overcome as our algorithms improve and as technology advances. In this regard, it is encouraging to note that prior to the last year or two, this type of investigation could never even be contemplated on less than mini or mainframe computer systems, and the computational costs would have been prohibitive. We fully expect computational technology developments to keep pace with scientific developments in modeling ERP and EEG phenomena.

Acknowledgement

The authors wish to thank Chris Larsen for her assistance with data collection.

References

Achim, A., Richer, F. and Saint-Hilaire, J.M. Methods for separating temporally overlapping sources of neuroelectric data. Brain Topogr., 1988a, 1: 22–28.

Achim, A., Richer, F., Alain, C. and Saint-Hilaire, J.M. A test of model adequacy applied to the dimensionality of multichannel average auditory evoked potentials. In: D. Samson-Dollfus (Ed.), Statistics and Topography in Quantitative EEG. Elsevier, Paris, 1988b: 161–171.

Ary, J.P., Klein, S.A. and Fender, D.H. Location of sources of evoked scalp potentials: Corrections for skull and scalp thicknesses. IEEE Trans. Biomed. Eng., 1981, 28: 447–452.

Brillinger, D.R. Some aspects of the analysis of evoked response experiments. In: M. Csorgo, D.A. Dawson, J.N.K. Rao and A.K.Md.E. Saleh (Eds.), Statistics and Related Topics, North-Holland Publ., Amsterdam, 1981: 155–168.

Brody, D.A., Terry, F.H. and Ideker, R.E. Eccentric dipole in a spherical medium: generalized expression for surface potentials. IEEE Trans. Biomed. Eng., 1973, 20: 141–143.

Darcey, T.M., Ary, J.P. and Fender, D.H. Methods for the localization of electrical sources in the human brain. In: H.H. Kornhuber and L. Deecke (Eds.), Progress in Brain Research, Vol. 54. Elsevier, Amsterdam, 1980: 128–134.

Donchin, E. and Heffley, E.F. Multivariate analysis of event-related potential data: a tutorial review. In: D. Otto (Ed.), Multidisciplinary Perspectives in Event-Related Brain Potential Research. U.S. Government Printing Office, Washington, DC, 1978: 555–572.

Fender, D. Source localization of brain electrical activity. In: A.S. Gevins and A. Rémond (Eds.), Methods of Analysis of Brain Electrical and Magnetic Signals. EEG Handbook, Vol. I, Elsevier Science, Amsterdam, 1987: 355–403.

Freeman, W.J. Mass Action of the Nervous System. Academic Press, New York, 1975.

Freeman, W.J. Measurement of cortical evoked potentials by decomposition of their wave forms. J. Cybern. Inform. Sci., 1980, 2: 44–56.

Freeman, W.J. Analytic techniques used in the search for the physiological basis of the EEG. In: A. Gevins and A. Rémond (Eds.), Handbook of Electroencephalography and Clinical Neurophysiology, Vol. 3A. Elsevier Biomedical Press, Amsterdam, 1985: Ch. 18.

Gasser, T. and Müller, H.G. Kernel estimation of regression functions. In: T. Gasser and M. Rosenblatt (Eds.), Smoothing Techniques for Curve Estimation. Springer, New York, 1979: 23–68.

Hart, J.D. and Wehrly, T.E. Kernel regression estimation using repeated measurements data. J. Am. Statist. Ass., 1986, 81: 1080–1088.

He, B., Musha, T., Okamoto, Y., Homma, S., Nakajima, Y. and Sato, T. Electric dipole tracing in the brain by means of the boundary element method and its accuracy. IEEE Trans. Biomed. Eng., 1987, 34: 406–414.

Henderson, C.J., Butler, S.R. and Glass, A. The localization of the equivalent dipoles of EEG sources by the application of electric field theory. Electroenceph. clin. Neurophysiol., 1975, 39: 117–130.

Homma, S., Nakajima, Y., Musha, T., Okamoto, Y. and He, B. Dipole-tracing method applied to human potentials. J. Neurosci. Meth., 1987, 21: 195–200.

Kavanagh, R.N., Darcey, T.M., Lehmann, D. and Fender, D.K. Evaluation of methods for 3-dimensional localization

of electrical sources in the human brain. IEEE Trans. Biomed. Eng., 1978, 25: 421–429.

Lehmann, D. and Skrandies, W. Spatial analysis of evoked potentials in man — a review. Prog. Neurobiol., 1984, 23: 227–250.

Lutzenberger, W., Elbert, T., Rockstroh, B. and Birbaumer, N. Principal component analysis of slow brain potentials during 6 second anticipation intervals. Biol. Psychol., 1981, 13: 271–279.

Maier, J., Dagnelie, G., Spekreijse, H. and van Dijk, B.W. Principal components analysis for source localization of VEPs in man. Vision Res., 1987, 27: 165–177.

Möcks, J. The influence of latency variations in principal component analysis of event-related potentials. Psychophysiology, 1986, 23: 480–484.

Möcks, J. Decomposing event-related potentials: a new topographic components model. Biol. Psychol., 1988a, 26: 199–215.

Möcks, J. Topographic components model for event-related potentials and some biophysical considerations. IEEE Trans. Biomed. Eng., 1988b, 35: 482–484.

Möcks, J. and Verleger, R. Principal component analysis of event-related potentials: a note on misallocation of variance. Electroenceph. clin. Neurophysiol., 1986, 65: 393–398.

Möcks, J., Köhler, W., Gasser, T. and Pham, D.T. Novel approaches to the problem of latency jitter. Psychophysiology, 1988, 25: 217–226.

Näätänen, R. and Picton, T. The N1 wave of the human electric and magnetic response to sound: a review and an analysis of the component structure. Psychophysiology, 1987, 24: 375–425.

Nunez, P.L. Electric Fields of the Brain. Oxford Press, New York, 1981.

O'Neill, R. Function minimization using a simplex procedure. Appl. Statist., 1971, 20: 338–345.

Priestley, M.B. Spectral Analysis and Time Series. Academic Press, London, 1981.

Raz, J., Turetsky, B. and Fein, G. Selecting the smoothing parameter for estimation of slowly changing evoked potential signals. Biometrics, 1989, 45: 745–762.

Rémond, A. The importance of topographic data in EEG phenomena, and an electrical model to reproduce them. Electroenceph. clin. Neurophysiol., 1968, Suppl. 27: 29–49.

Rösler, F. and Manzey, D. Principal components and varimax-rotated components in event-related potential research: some remarks on their interpretation. Biol. Psychol., 1981, 13: 3–26.

Scherg, M. Fundamentals of dipole source potential analysis. In: M. Hoke, F. Grandori and G.L. Romani (Eds.), Auditory Evoked Magnetic Fields and Potentials. Karger, Basel, 1989.

Scherg, M. and Von Cramon, D. Two bilateral sources of the late AEP as identified by a spatio-temporal dipole model. Electroenceph. clin. Neurophysiol., 1985, 62: 32–44.

Scherg, M. and Von Cramon, D. Evoked dipole sources of the human auditory cortex. Electroenceph. clin. Neurophysiol., 1986, 65: 344–360.

Skrandies, W. and Lehmann, D. Spatial principal components of multichannel maps evoked by lateral visual half-field stimuli. Electroenceph. clin. Neurophysiol., 1982, 54: 662–667.

Squires, N.K., Squires, K.C. and Hillyard, S.A. Two varieties of long-latency positive waves evoked by unpredictable auditory stimuli in man. Electroenceph. clin. Neurophysiol., 1975, 38: 387–401.

Turetsky, B., Raz, J. and Fein, G. Noise power and signal power and their effects on evoked potential estimation. Electroenceph. clin. Neurophysiol., 1988, 71: 310–318.

Wood, C.C. Application of dipole localization methods to source identification of human evoked potentials. In: I. Bodis-Wollner (Ed.), Evoked Potentials. New York Academy of Sciences, New York, 1982: 139–155.

Wood, C.C. and McCarthy, G. Principal component analysis of event-related potentials: simulation studies demonstrate misallocation of variance across components. Electroenceph. clin. Neurophysiol., 1984, 59: 249–260.